In vitro selection of a viomycin-binding RNA pseudoknot

Mary G Wallis[1], Barbara Streicher[1], Herbert Wank[1]*, Uwe von Ahsen[1†], Elisabeth Clodi[1], Scot T Wallace[1], Michael Famulok[2] and Renée Schroeder[1]

Background: The peptide antibiotic viomycin inhibits ribosomal protein synthesis, group I intron self-splicing and self-cleavage of the human hepatitis delta virus ribozyme. To understand the molecular basis of RNA binding and recognition by viomycin, we isolated a variety of novel viomycin-binding RNA molecules using *in vitro* selection.

Results: More than 90% of the selected RNA molecules shared one continuous highly conserved region of 14 nucleotides. Mutational analyses, structural probing, together with footprinting experiments by chemical modification, and Pb^{2+}-induced cleavage showed that this conserved sequence harbours the antibiotic-binding site and forms a stem–loop structure. Moreover, the loop is engaged in a long-range interaction forming a pseudoknot.

Conclusions: A comparison between the novel viomycin-binding motif and the natural RNA target sites for viomycin showed that all these segments form a pseudoknot at the antibiotic-binding site. We therefore conclude that this peptide antibiotic has a strong selectivity for particular RNA pseudoknots.

Addresses: [1]Institute of Microbiology and Genetics, University of Vienna, Dr. Bohrgasse 9, A-1030 Vienna, Austria. [2]Institute of Biochemistry, Genzentrum of the Ludwig-Maximilian-University of Munich, Würmtalstrasse 221, D-81375 Munich, Germany.

Present addresses: *Department of Molecular Genetics, Ohio State University, 484 West 12th Avenue, Columbus, Ohio 43210, USA. †Research Institute of Molecular Pathology, Dr. Bohrgasse 7, A-1030 Vienna, Austria.

Correspondence: Renée Schroeder
E-mail: renee@gem.univie.ac.at

Key words: antibiotics, *in vitro* selection, RNA aptamers, RNA pseudoknots, viomycin

Received: **30 January 1997**
Revisions requested: **18 February 1997**
Revisions received: **25 March 1997**
Accepted: **1 April 1997**

Chemistry & Biology May 1997, 4:357–366
http://biomednet.com/elecref/1074552100400357

Introduction

Numerous antibiotics interact with RNA, as confirmed by a plethora of observations over many years. Interactions of antibiotics with the ribosome have been the focus of such antibiotic studies [1] and more recently, group I introns have been shown to interact with a multitude of chemically different small molecules, including structurally diverse antibiotics from the aminoglycoside [2,3], peptide [4], and pseudodisaccharide families [5]. Generally, these antibiotics inhibit RNA function, but in two cases the peptide antibiotics from the tuberactinomycin family stimulate RNA activity. In the first case, viomycin enhances the cleavage reaction of the ribozyme derived from the *Neurospora crassa* VS RNA [6]. In the second, both disruption of the self-splicing activity of group I introns [4] and the induction of intron oligomerization [7] have been shown to occur in the presence of viomycin. Recently, it was reported that viomycin inhibits the self-cleavage activity of the human hepatitis delta virus (HDV) ribozyme [8].

Our aim is to understand the principles underlying binding and recognition of antibiotics by RNA. Many pathogen-specific RNA molecules are inhibited by antibiotics (reviewed in [9]) and retrovirus-derived diseases are in urgent need of therapy. The development of novel drugs targeted against pathogen-specific RNA molecules requires a detailed understanding of the interactions between RNA and small molecules.

In vitro selection and evolution has allowed the exploration of many facets of RNA activity including the identification of unique binding and catalytic properties (reviewed in [10]). We sought to investigate the fundamental nature of antibiotic–RNA interactions with a view to understanding the manner in which antibiotics disturb intrinsic RNA functions. The possibility that the specific recognition of RNA molecules by antibiotics implicates common structural targets has recently been investigated for a variety of aminoglycoside antibiotics. Three independent studies sieved different random-sequence pools for RNA molecules which specifically bound neomycin [11], tobramycin [12], kanamycin A or lividomycin [13]. *In vitro* selection led to the isolation of small RNA molecules which were amenable to molecular characterization, in contrast to the 'classic' biological RNA molecules which, owing to their size, often require dissection before structural information is accessed [14–16].

In this study, we used *in vitro* selection to isolate aptamers which specifically recognize the peptide antibiotic

Figure 1

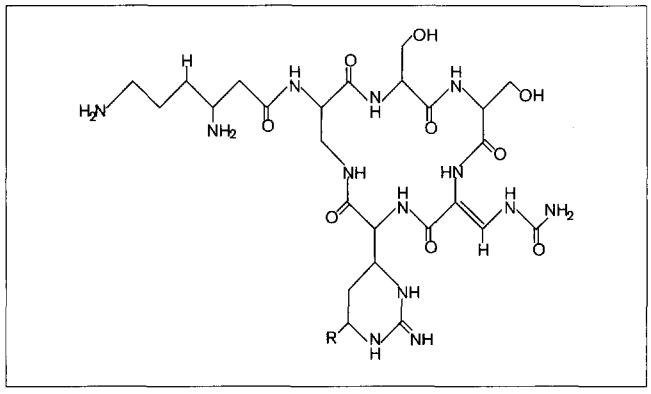

The cyclic peptide antibiotic viomycin (R=OH) and its analogue tuberactinomycin O (R=H).

viomycin. Characterization of these small molecules showed that almost all the selected RNA molecules contained a region of highly conserved sequence. This 'consensus' region was shown to contribute to the formation of a pseudoknot structure and to harbour the site of interaction with viomycin.

The knowledge that resistance to antibiotics provides a relentless threat [17] gives substantial impetus to attempts to advance our understanding of antibiotic 'behaviour', including antibiotic–RNA interactions. Our studies provide an insight into certain structural fundamentals underlying these interactions and they demonstrate that *in vitro* selection is an appropriate tool for the isolation of synthetic receptors.

Results

Isolation of viomycin-binding RNA molecules

Using *in vitro* selection, we isolated novel RNA molecules which specifically recognize the cyclic peptide antibiotic viomycin (Figure 1). The initially randomized RNA pool, of approximate complexity 10^{15}, comprised molecules containing a 74 nucleotide core of random sequence [18]. This pool was subjected to seven cycles of viomycin-affinity chromatographic selection: RNA molecules specifically retained on the antibiotic-derivatized sepharose column were affinity-eluted with selection buffer containing 2.5 mM viomycin. The course of the selection is summarized in Table 1. In order to enrich the pool with a more homogeneous population of molecules, the number of washes prior to affinity elution was increased from the fourth cycle onwards. By the seventh selection cycle, the percentage of viomycin-binding RNA molecules that could be eluted had reached saturation.

After seven cycles of selection, the RNA population that had been successively enriched with molecules recognizing viomycin was cloned as described previously [11] and the sequences of individual clones were determined. The variability of the sequences was high: in a total of 23 different sequences only one was isolated repeatedly (vio118, six times), but over a short stretch of 14 nucleotides ($5'G_1C_2$-$U_3G_4A_5A_6A_7G_8G_9A_{10}U_{11}C_{12}G_{13}C_{14}3'$), the different clones were closely related at the primary sequence level (Figure 2). In this highly conserved consensus sequence, eight invariant bases and two nonconserved bases occurred ($A_6 \rightarrow G$ in three out of 21 clones and $A_7 \rightarrow C$ in two cases). At both the 5′ and 3′ extremities of the conserved sequence two covariant bases suggested that a stem structure closes the motif. In addition to the conserved sequence, bases in the regions upstream and downstream of this consensus sequence had the potential to pair, thus leading us to propose a stem–loop structure for the motif (Figure 3).

Table 1

Viomycin *in vitro* selection summary.

Selection cycle number	Number of buffer washes	Number of affinity washes	RNA affinity-eluted (%)
1	5	2	0.02
2	5	2	0.25
3	5	2	0.25
4	5	2	19
4 bis	30	2	1.5
5	40	2	6.3
6	30	2	22
7	30	2	23

Selection cycles and number of buffer washes prior to the viomycin-affinity washes are indicated, where one wash represents one column volume. The progression of the selection was monitored by determining the percentage (%) of the input RNA which was affinity-eluted with viomycin from the antibiotic-derivatized chromatography column. Cycle 4 bis is the repetition of cycle 4 with an increased number of washes.

Determination of K_d for individual clones

From the enriched RNA pool, the viomycin-binding behaviour of several representative clones was determined. Individual RNA molecules were chosen on the basis of the primary sequence variation within the conserved motif and on the position of this motif within the full-length clone. The ability of individual clones to recognize viomycin specifically was verified by affinity chromatography, and all RNA molecules tested showed similar affinity for viomycin. Gel filtration analysis using ^{14}C-labelled viomycin was used to determine the dissociation constants (K_ds) for antibiotic binding in solution. The dissociation constants for RNA molecules matching the consensus sequence fell into the range 11–21 μM (Table 2).

Probing the structure of *in vitro* selected RNA molecules and their interaction with viomycin

Folding of the individual full-length sequences using the Zuker RNA-folding program [19] and the covariation shown

Figure 2

vio1: ggagcucagccuucacugcugaaaggaucgcaggauggacucugcuaucggacugaagccaguugguggucagcccacaugcggaggguucccggcaccacggucggauccac
vio2: ggagcucagccuucacugcaccgguggcguguggccuagcuccaggccaaguuguggcgaugaaaggaucuuuccacagcagaggugcucuuuggcaccacggucggauccac
vio3: ggagcucagccuucacugcguagcgcguauuggcugcgacugaaaggaucgucgcaagagaguccuccaugaucggcaccacggucggauccac
vio9: ggagcucagccuucacugcucaagcaaaucugccgcucagcugagaggaucgcuguugguagguguagaagguacuauaggcaccgcgauuguggcaccacggucggauccac
vio12: ggagcucagccuucacugccucagggcgggugaagggugcugaaaggaucgcacuucuaaaaggccauguguagccaccacugaugugggcgcggcaccacggucggauccac
vio15: ggagcucagccuucacugcuagugaagguuugggaaccgggcugaaaggaucgccacugaccaauucaguuggucuacgaucgucgccgaaaacggcaccacggucggauccac
vio22: ggagcucagccuucacugcugaaaggaucgcaguuaaacagcgacguggugcaauagcggggugggaacugccgucaguucuccaucucguugggcaccacggucggauccac
vio24: ggagcucagccuucacugcauggcggcugaggcggcacugaaaggaucgucccgcguuauuccuucggccguagucuggcaccacggucggauccac
vio52: ggagcucagccuucacugcgagcguuggcugagugcucugcugaacggaucgcagagcagcugccugugcaacggcaaucuguuguacugcaggcaccacggucggauccac
vio74: ggagcucagccuucacugcauuggcugaguuaguguguguugaaaggaucacaacgcuacgcgggaaacugcaugacuuaaugauaugcgguggcaccacggucggauccac
vio109: ggagcucagccuucacugcuagugagggcaacuucgauuagcugaaaggaucgcuucggaggaccagcgagcuccgugauuguggcagcuaguggcaccacggucggauccac
vio111: ggagcucagccuucacugcugagaggaucgcgguaaggugugggcgaacagucgaaugcggcacguucaccauagagagcucccgaucggcaccacggucggauccac
vio112: ggagcucagccuucacugcuaugcugaaaggaucgcauagcuguuuaggugauuauaccaccuggacugucucuccaguggccgagguugcuuggcaccacggucggauccac
vio113: ggagcucagccuucacugcauaggugggggguagcugaaaggaucgcuagcuccaaggccgcggugcaucaaucccuggggcuaugggguucguuggcaccacggucggauccac
vio114: ggagcucagccuucacugcugaacggaucgcuaugaaggaacagggugaaaaccuagaaaucauugagcugcgcggccaugggacucauccgaggcaccacggucggauccac
vio118: ggagcucagccuucacugcuguagcgcauuacgccggugggagacugauagaucgguggacaucgccccuggaacaccgcaaguccaggauguaggcaccacggucggauccac
vio120: ggagcucagccuucacugcugaaaggaucgcaguaaagaccguguaaccggcuugaaaauguauaaaccuaacgaacuuauaccacaucaucuggcaccacggucggauccac
vio125: ggagcucagccuucacugcacguucccccucauaucgaggggauaacuauagugcaggugcugaaaggaucgcacucccaggccgggugguuuggcaccacggucggauccac
vio127: ggagcucagccuucacugcgacaaggcaguggauguguuuacgcaccacacguggacugacauaagcugaaaggaucgcuaguccacaaccguggcaccacggucggauccac
vio128: ggagcucagccuucacugccgacuguaggccguaacugaucggcgcaaaggaaggaacgauuggcuauaaaguagccuaaguucugugcugcaaggcaccacggucggauccac
vio129: ggagcucagccuucacugcagggcaagcugagaggaucgcuaugcuccacgaccgucagugccuaggaaaggcuguauguauacgcuuagcuuggcaccacggucggauccac
vio130: ggagcucagccuucacugccugaaaggaucggcagucaaugaccggagaggugucaugacgaaaacgggagaaacuaauuagugccucccgacggcaccacggucggauccac
vio145: ggagcucagccuucacugcaauggccgcuagguugaugugcagugaagucagcugaggcccagggcugaaaggaucgccuccucgacucguggcaccacggucggauccac

The primary sequence of 23 individual clones comprising the pool after the seventh cycle of selection. The clone number is shown on the left. The sequences shown represent the full-length RNA molecules in the originally degenerate core region (74 nucleotides) plus the defined flanking regions that enable primer binding. Nucleotides matching the consensus sequence are shown in bold and in block shading.

in Figure 3 suggest that the region of primary homology forms a stem–loop secondary structure. Chemical modification was undertaken to determine whether individual RNA molecules formed the proposed stem–loop motif represented by the computer generated folding, to examine whether the primary sequence covariations (mentioned above) indeed reflected a conserved structural feature, and to localize the regions within individual selected clones which interact with viomycin.

RNA clones vio74, vio130 and vio145 (see Figure 2) were selected for further characterization and the chemical modification agents dimethyl sulphate (DMS), kethoxal or 1-cyclohexyl-(2-morpholinoethyl)-carbodiimide metho-*p*-toluene sulphonate (CMCT) were used specifically to modify accessible bases [20]. Positions on the full-length RNA molecules that could be modified were revealed by primer extension of an annealed oligonucleotide. A typical modification pattern is shown in Figure 4 for the clone vio145. The secondary structure proposed by the Zuker RNA folding algorithm and the chemical modification pattern of the RNA molecules (in the absence of antibiotic) were generally in agreement (i.e. the computer-predicted base-paired regions were protected from modification). The chemical modification data suggested that bases G_1

Figure 3

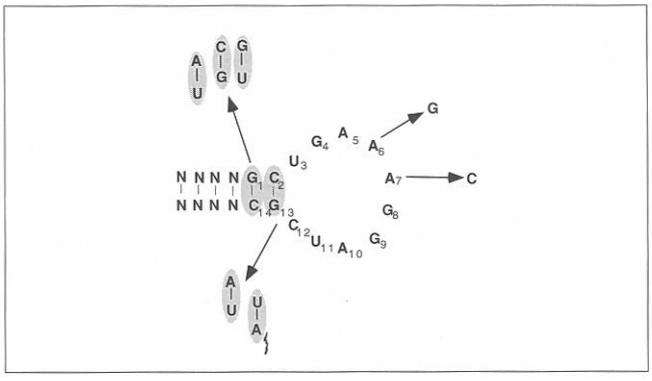

Variations of the consensus sequence proposing a stem–loop structure.

Table 2

Summary of the dissociation constants (K_ds) for the binding of viomycin to selected RNA molecules.

Aptamer	Motif feature	K_d (μM)
vio112	Consensus	11.6±2
vio145	Consensus	13.1±6
vio74	Stem C2G13 to UA	12.6±2
vio130	Stem G1C14 to CG	15.9±3
vio111	Loop A6 to G	21.0±3
vio52	Loop A7 to C	15.0±4

The numbering scheme for the conserved sequence motif is as follows: 5′ $G_1C_2U_3G_4A_5A_6A_7G_8G_9A_{10}U_{11}C_{12}G_{13}C_{14}$ 3′. The K_d measurements were determined for the full-length clones. The K_d values were calculated from at least three independent experiments.

Figure 4

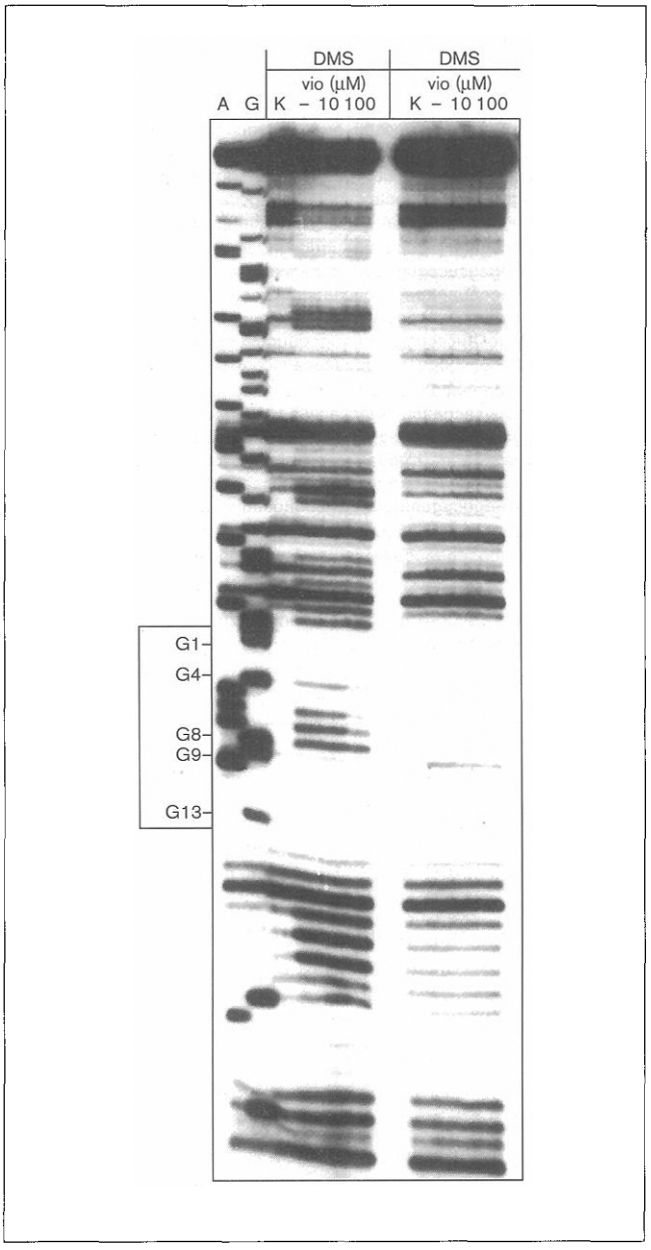

Chemical modification of the selected RNA vio145, in the presence and absence of viomycin. For the specificities of the chemically modifying agents see the Materials and methods section. A (adenine) and G (guanine) denote dideoxy sequencing lanes (note that in the sequence lane, the bands are one nucleotide longer than in the corresponding chemical modification lane, because after modification the corresponding nucleotide is no longer incorporated by the reverse transcriptase). K, control (i.e. no modification); –, no viomycin; otherwise the antibiotic concentrations were 10 μM and 100 μM as shown.

and C_2 paired with C_{14} and G_{13}, respectively, an interaction that is corroborated by sequence covariation (Figure 3). The Watson–Crick positions of U_3 were not accessible to modification with CMCT but were modified by DMS (Figure 4 and data not shown). Positions N1 and N2 of G_4 were not accessible to kethoxal modification. Positions A_5–A_7 were modified by DMS and G_8 was modified by kethoxal (Figure 4). Positions G_9–C_{12} were not accessible to modification, suggesting that they are involved in base pairing.

Chemical modification of the native RNA structures complexed with 10 μM or 100 μM viomycin was also undertaken. Four adjacent positions clearly showed protection by viomycin against modification from DMS (Figure 4 and data not shown). These positions are located in the loop of the conserved sequence: the unusually modified U_3, position N7 of G_4 and position N1 of A_5 and A_6. The N1 and N2 positions of G_8, modifiable by kethoxal, were also protected by viomycin. All the RNA molecules tested revealed a similar 'footprint' of protected bands, which was solely located within this conserved motif. Consistent with the idea that invariant positions in RNA molecules are potentially indicative of 'functional bases', the protection afforded by viomycin is notably stronger at G_4 and A_5 than at A_6. Interestingly, these two bases are at positions which are absolutely conserved among the selected RNA molecules bearing the consensus sequence (Figures 2,3). Variant vio111, which has an $A_6 \rightarrow G$ mutation, has a lower affinity for viomycin than the clones which completely match the consensus sequence at these positions (Table 2).

Pb^{2+}-induced cleavage of viomycin-binding RNA molecules

In addition to the chemical modification analysis, we used Pb^{2+}-induced RNA cleavage to probe the structures of our novel viomycin-binding RNA molecules and to analyze their interaction with viomycin. Cleavage was induced in 5′ ^{32}P-labelled RNA molecules upon exposure to $Pb(OAc)_2$ under the conditions described in the Materials and methods section [21]. Cleavage positions were identified by comparison with a T1 digestion ladder (see Materials and methods section). Figures 5a and 5b show representative analyses for the selected clones vio130 and vio145, respectively. Pb^{2+}-induced cleavage occurred predominantly at phosphate positions in single-stranded regions. This correlates well for each case (clones vio74, vio130 and vio145) with the secondary structures proposed by the Zuker RNA folding algorithm and by chemical modification. The cleavage pattern shows that not all the backbone positions within the loop are equally accessible. Two sites exist at which strong cleavage occurs readily: 3′ of A_7 and U_{11}. Although Pb^{2+} preferentially hydrolyzes single-stranded RNA, cleavage may occur in double-stranded regions if they contain weak, bulged or destabilized base pairs. In addition to the major sites of cleavage, several contiguous positions of moderate or weak cleavage occur which correspond to the region of the loop at which a footprint by viomycin is observed. The presence of numerous adjacent Pb^{2+}-cleavage sites has been proposed to reflect a region of high flexibility [21]. Another remarkable feature

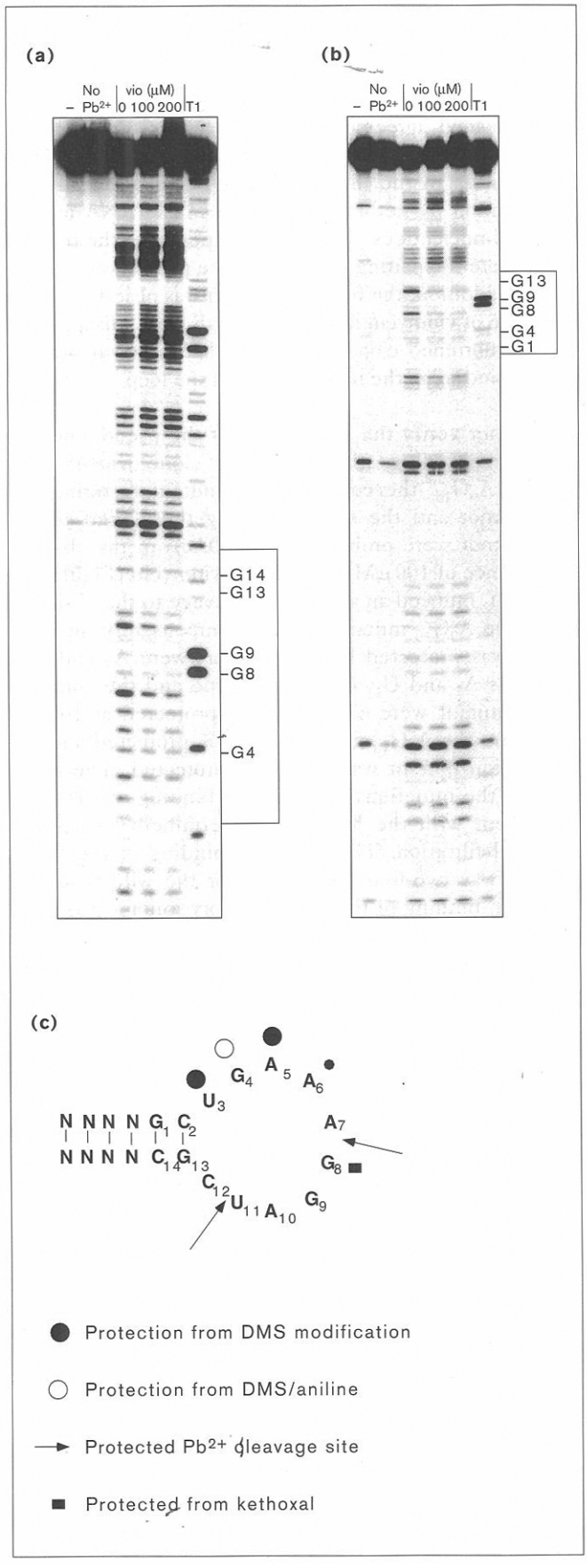

of this loop structure appears to be the region of the backbone G_8–A_{10}, where the phosphates show extremely low accessibility to Pb^{2+}-promoted hydrolysis. This suggests that this side of the loop may be involved in a structural interaction which protects these three phosphate positions. Identical cleavage patterns within this consensus region were observed in individual RNA aptamers, suggesting a common structural feature of the conserved motif. Taken together, the Pb^{2+}-cleavage analyses corroborate the structural conclusions of the chemical modification analyses, supporting the idea of an irregular stem–loop motif.

The Pb^{2+}-cleavage assay was carried out in the presence of viomycin in an attempt to identify the viomycin-binding site within the full-length RNA molecules and to test whether there were any structural changes upon viomycin–RNA complex formation. Viomycin protected several positions in the conserved consensus region from cleavage, as seen in the Pb^{2+}-induced hydrolysis pattern (Figure 5a,b and data not shown). The most dramatic effect was seen at phosphate positions to the 3′ side of A_7 and U_{11}, where the cleavage was strongly inhibited in the presence of 100 μM viomycin. The position 3′ of C_{12}, which showed a moderate cleavage signal, was also protected upon addition of viomycin. These results show that the binding of the peptide antibiotic viomycin to the *in vitro* selected RNA molecules protects certain backbone positions which are located within the consensus motif. The protection may either be the result of a direct interaction of the antibiotic with specific phosphates and/or it may result from the loss of flexibility of the backbone upon viomycin binding. Figure 5c summarizes the results obtained from chemical modification and Pb^{2+}-cleavage.

The high degree of sequence conservation, the results of chemical modification and the Pb^{2+}-cleavage data encouraged us to construct a short oligoribonucleotide consisting of the conserved loop with a stem containing six base pairs (data not shown). This short RNA was tested in a Pb^{2+}-cleavage assay in the absence and presence of viomycin to test whether the Pb^{2+}-cleavage pattern would reflect a

Figure 5

Structural probing of the viomycin-binding RNA molecules with $Pb(OAc)_2$ in the absence and presence of viomycin. The cleavages were carried out in buffer containing 200 mM NaCl and 5 mM $MgCl_2$. Lanes marked '–' and 'no Pb^{2+}' contain non-incubated and incubated RNA, respectively, in the absence of $Pb(OAc)_2$. Pb^{2+}-induced cleavage was performed in the presence of various concentrations of viomycin as indicated above the corresponding lane. T1 represents the partial RNAse T1 digestion, with cleavage positions at the 3′ side of preferentially single-stranded guanine bases. The nucleotide numbering scheme is based on the conserved sequence motif as follows: 5′ $G_1C_2U_3G_4A_5A_6A_7G_8G_9A_{10}U_{11}C_{12}G_{13}C_{14}$ 3′. **(a)** RNA derived from clone vio130. **(b)** RNA derived from clone vio145. **(c)** Summary of protections from chemical modification and Pb^{2+} cleavage by viomycin in the consensus region.

structure similar to the full-length clone and whether the same protection would appear with viomycin. The short construct showed a similar Pb^{2+}-cleavage pattern with the strongest cleavage at positions A_7 and U_{11}. But positions G_8–A_{10} were much more sensitive to Pb^{2+} cleavage than in the full-length construct. Viomycin still protected the cleavage at position A_7, although it was tenfold less efficient than for the full-length clone. The cleavage at U_{11} was not protected by viomycin (data not shown). From these results we concluded that the conserved stem–loop alone is not sufficient to achieve full viomycin-binding activity.

Interference studies suggest that the conserved motif is not sufficient for binding

To determine the minimal motif capable of high-affinity binding of viomycin, individual RNA molecules were partially hydrolyzed (as described previously [11]) and then subjected to affinity chromatography. RNA molecules that retained binding capability were affinity-eluted and compared with total non-selected partially hydrolyzed RNA molecules. These experiments confirmed that the hairpin motif alone is not sufficient for binding. Although all clones tested could be shortened from the 5′ side, none of the clones tolerated shortening from the 3′ side (data not shown). From these observations, we concluded that the extreme 3′ end of the molecules is essential for viomycin binding. The bases in the 3′ terminal sequence 5′GAUCC3′, which is part of the invariant flanking sequence that provides primer binding sites for amplification, have the potential to pair with bases G_8–C_{12} of the conserved motif.

Mutational analyses identify a pseudoknot motif for viomycin recognition

All the clones contain a 5′GAUCC3′ sequence, which is part of the invariant primer used for amplification and which has the potential to base pair with sequences within the conserved loop. We tested whether these sequences do indeed undergo base pairing. The following variants of clone vio145 were constructed: positions G_9 and A_{10} in the conserved loop were mutated to A_9 and G_{10} and the 3′ terminal sequence 5′GAUCC3′ was mutated to 5′GACUC3′, both of which should disrupt the suspected pairing; and a compensatory combination of both mutants, which should restore the pairing. The K_d values of the wild-type clone vio145 and the three variants were determined by gel filtration analysis. The results are shown in Figure 6a. The variants which disrupt the potential base-pairing have an almost twofold lower affinity for viomycin, whereas the compensatory mutation restores binding affinity almost to the wild-type level. These experiments suggest that the 3′ terminal sequence 5′GAUCC3′ interacts with the sequence 5′GGAUC3′ in the conserved loop, which results in the formation of a pseudoknot.

The formation of the pseudoknot was further tested by constructing a variant of clone vio145 which lacked the last six nucleotides, five of which are thought to form the pseudoknot. This RNA was analyzed by chemical modification with DMS and kethoxal in the absence or presence of viomycin (Figure 6b). The results from this experiment were in good agreement with the results of Figure 6a. Positions G_9, A_{10} and C_{12}, which were not accessible to modification in the full-length RNA, were accessible to modification by kethoxal and DMS in the RNA lacking the final nucleotides. This was as expected if the missing bases were the pairing partners for the pseudoknot formation. In addition, the footprint, which was observed in the presence of viomycin in the full-length RNA, disappeared in the shortened clone, indicating that viomycin was no longer binding to the region U_3–A_6 of the loop.

To further verify the importance of the pseudoknot for viomycin binding, the wild-type clone vio145, the mutant A_9G_{10}, the compensatory mutant restoring the pseudoknot and the variant lacking the 3′ part of the pseudoknot were probed with $Pb(OAc)_2$ in the absence or presence of 100 μM and 200 μM viomycin (Figure 6c). $Pb(OAc)_2$ induced an additional cleavage to the 3′ side of G_8 in the A_9G_{10} mutant and the compensatory mutants, which was protected by viomycin as were A_7 and U_{11}. Positions A_7 and U_{11} of the wild-type and the compensatory mutant were 67% and 60% protected at 100 μM viomycin, the A_9G_{10} mutant was 33% protected and the 3′ deletion mutant was only 12% protected. The influence of the mutations on viomycin binding was in good agreement with the K_d values determined via equilibrium gel filtration. The viomycin binding of the A_9G_{10} mutant was two-fold lower than for the wild-type; the viomycin binding of the compensatory mutant was comparable to that of the wild-type; and the viomycin binding of the 3′ deletion totally lacking the pseudoknot was almost ten-fold lower.

These data are consistent with the formation of a pseudoknot which is essential for viomycin binding, and the proposed secondary structure of clone vio145 is given in Figure 6d.

Discrimination between viomycin and its analogue tuberactinomycin O

To get an idea of whether the selected motif binds viomycin in a similar way to the self-splicing group I intron, the viomycin analogue tuberactinomycin O, which is not an inhibitor of splicing [4], was tested for its binding to the clone vio145. Clone vio145 was analyzed by Pb^{2+} cleavage in the presence of 200 μM viomycin or tuberactinomycin O. As can be seen from Figure 7, viomycin strongly protects positions A_7 and U_{11} from Pb^{2+} cleavage, whereas tuberactinomycin O does not. This is a first indication that the hydroxyl group, which is missing in tuberazctinomycin O, is essential for binding to the *in vitro* selected RNA pseudoknot, as it is for inhibiting splicing.

Discussion

Viomycin, a small cyclic peptide antibiotic (Figure 1), specifically recognizes a diverse set of highly structured, functional RNA molecules. To achieve a better understanding of the minimal requirements governing viomycin–RNA interactions, we aimed to isolate and characterize small recurring motifs recognized by viomycin, which would be amenable for structural determination.

Our selection identified one commonly recurring motif, a pseudoknot, which is important for binding viomycin. The population of viomycin-binding RNA molecules

Figure 6

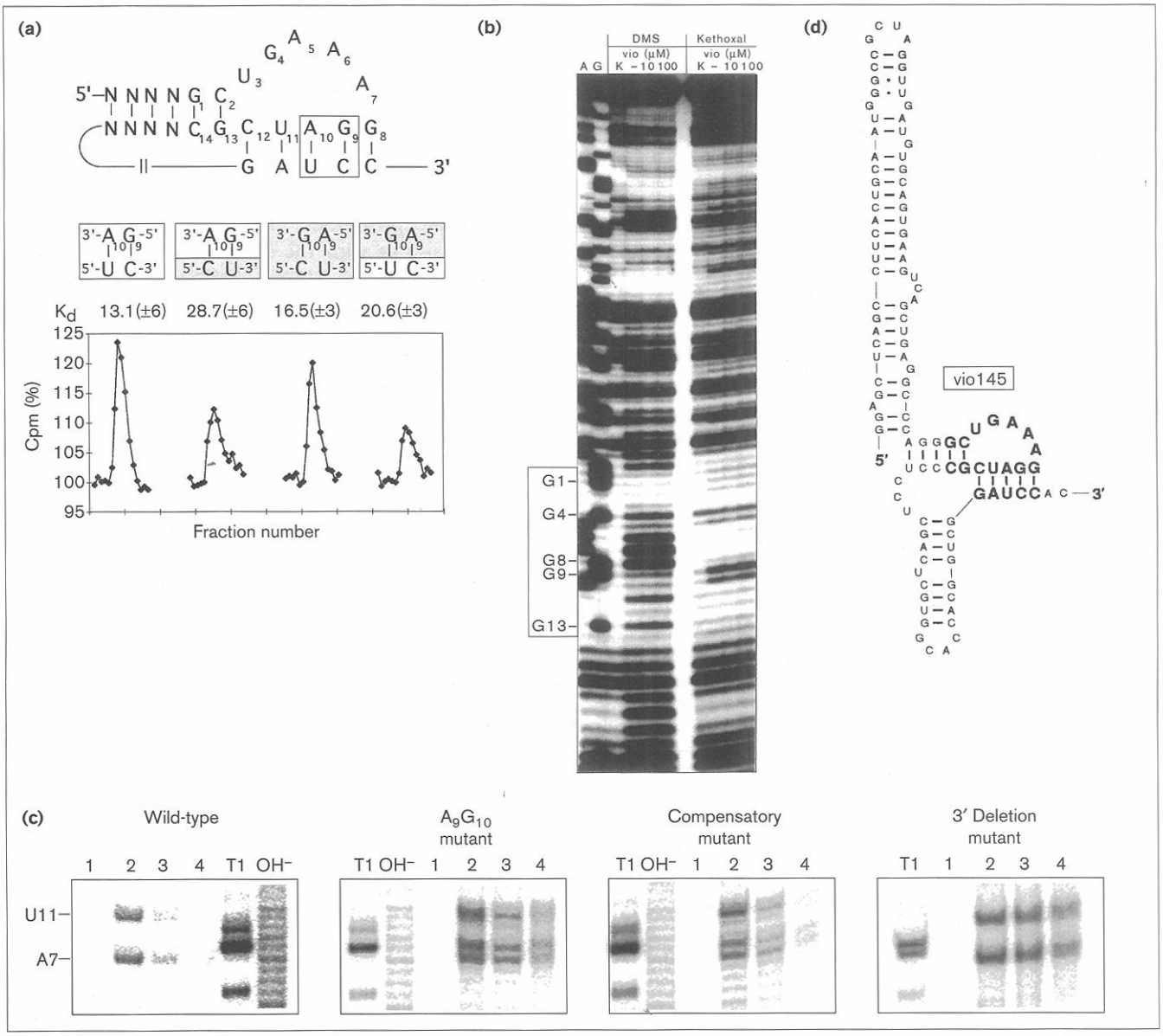

Determination of K_d values for variants of clone vio145 disrupting and restoring the proposed long-range interaction. **(a)** Equilibrium gel filtration determination of the K_d value for vio145 with ^{14}C-viomycin in solution. The figure shows the relative radioactivity (where 100% is the activity of the running buffer) versus the fraction number (39.4 μl). The peak corresponds to the viomycin–RNA complex. **(b)** Chemical modification of a variant of clone vio145 lacking the last six nucleotides, resulting in the disruption of the proposed pseudoknot. Lane annotations and experimental procedures are as described in Figure 4. **(c)** Footprinting viomycin interactions with variants of clone vio145. Mutant A_9G_{10}, the compensatory mutant which restores the pseudoknot, and the variant lacking the 3′ part of the pseudoknot were incubated with $Pb(OAc)_2$ in the absence (lane 2) or in the presence of 100 μM (lane 3) or 200 μM (lane 4) viomycin. T1 is the partial RNase T1 digestion, OH^- the partial alkaline hydrolysis ladder, and lane 1 is RNA only. **(d)** Proposed secondary structure of clone vio145 with the pseudoknot.

Figure 7

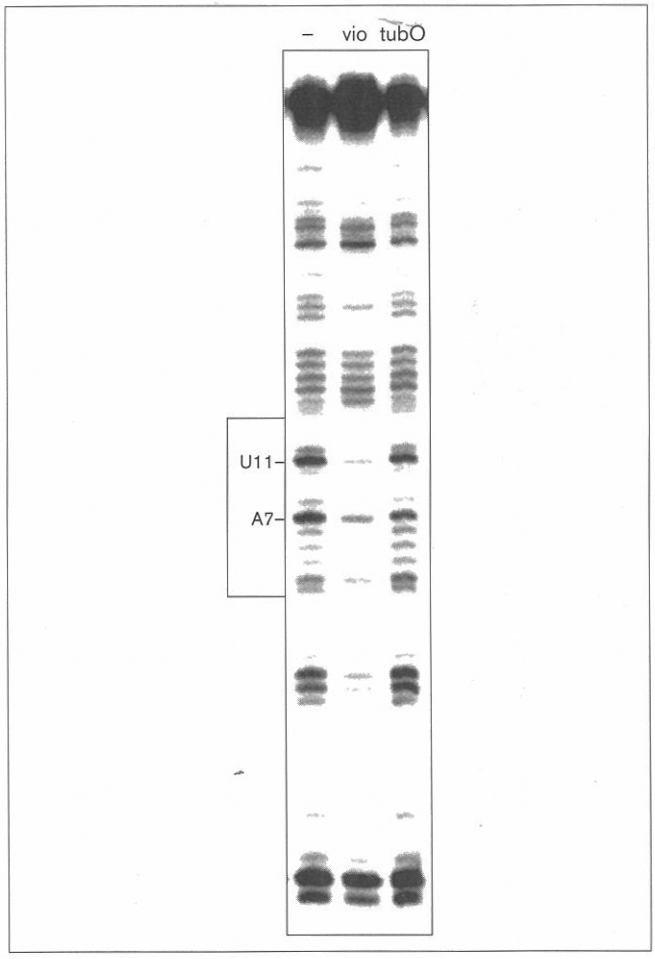

Clone vio145 was tested for discrimination between viomycin and tuberactinomycin O (see Figure 1). $Pb(OAc)_2$ cleavage was done in the absence or presence of 200 μM viomycin or tuberactinomycin O (see Figure 5).

obtained from our selection shows a remarkable homogeneity, not only reflected in their sequence motif but also in their K_d values for viomycin (see Table 2). Most RNA molecules have $K_d = 11–16$ μM viomycin, one clone (vio111), however, has a lower affinity (21 μM), which could be explained by the variation in the consensus sequence ($A_6 \rightarrow G$; a position shown to be protected by viomycin from DMS modification; Figures 4,5c). The binding constants for the *in vitro* selected RNA molecules are comparable with interactions observed for natural viomycin–RNA complexes. Viomycin inhibits group I intron self-splicing at 17–50 μM (depending on the intron [4]) and the HDV genomic and antigenomic ribozymes at 35 μM and 100 μM, respectively [8]. It must be taken into consideration, however, that these are K_i and not K_d values, and that the ionic conditions under which they were determined were not uniform.

The selection procedure resulted in the isolation of one dominant sequence motif (Figure 2) with the consensus 5′GCUGAAAGGAUCGC3′. The secondary structure of the motif is a stem–loop, the stem of which is corroborated by structural covariation and by chemical modification (Figures 3,4). The loop is not unstructured and is involved in a long-range interaction with sequences near the 3′ end of the RNA, resulting in the formation of a pseudoknot. While the 5′ half of the loop is accessible to modification, the 3′ part is not, suggesting that positions G_8–C_{12} are pairing with the distal 3′ end. By removing the last six nucleotides at the 3′ end of the RNA, positions G_9, A_{10} and C_{12} become accessible to modification (Figure 6b). Unusual features of the loop involve the DMS modification of U_3 and the inaccessibility of the N1 and N2 positions of G_4 to kethoxal. Bases U_3 and G_4 might be protected by the deep groove of the helix formed between positions G_8–C_{12} with the 3′ distal sequence 5′GAUCC3′. This is consistent with the structure of single-stranded loops in pseudoknots [22,23]. DMS does not usually modify uridines, but a high pH value has been shown to result in the modification of uridines by DMS [24]. The microenvironment of U_3 might result in this modified behaviour with respect to DMS. Positions A_7 and U_{11} show a high sensitivity to Pb^{2+} cleavage, which might result from a high flexibility of the backbone [21] or from a high-affinity metal ion binding site [25]. Addition of viomycin to the RNA results in protection of positions U_3 to A_6 from chemical modification and protection of positions A_7 and U_{11} from Pb^{2+} cleavage. These protections clearly demonstrate that this region of the RNA molecule harbours the viomycin-binding site.

Viomycin has the remarkable characteristic of inducing RNA–RNA interactions. Several reports underline this fact: viomycin stimulates oligomerization of group I intron RNA by shifting the intramolecular circularization to an intermolecular transesterification leading to intron-multimers [7]; the cleavage reaction of the ribozyme derived from *N. crassa* VS RNA is enhanced by viomycin, which decreases the required Mg^{2+} concentration by an order of magnitude and stimulates a *trans*-cleavage reaction [6]; viomycin has a binding site on each ribosomal subunit of the *Escherichia coli* ribosome [26,27] and it inhibits subunit dissociation and translocation [28,29]; and viomycin interferes with binding of the ternary complex to the ribosomal A site for codon–anticodon interactions containing a mismatch. It was concluded that viomycin increases the binding of mismatched codon–anticodon pairs by providing the same amount of binding energy as a base pair [30]. All these observations suggest that viomycin has more than one contact site with the RNA, a characteristic which results in a stimulation of intermolecular RNA interactions or in the stabilization of the tertiary structure. This characteristic is reminiscent of the mode of binding of another peptide antibiotic,

thiostrepton, which bridges two loops of domain II of 23S rRNA [16].

The result of our selection prompted us to compare the natural viomycin target sites with our novel pseudoknot motif; all those that have been characterized fold into a pseudoknot structure. Viomycin protects positions A_{913}–A_{915} of the 16S ribosomal RNA of *E. coli* from DMS modification. Positions immediately to the 3′ side of A_{915}, namely U_{916}–A_{918}, interact with positions U_{17}–A_{19} forming the central pseudoknot of 16S rRNA, which has been suggested to be involved in the regulation of translation accuracy [26,31]. Positions 913–915 of the 16S rRNA are three consecutive adenines. In the pseudoknot isolated via *in vitro* selection, three consecutive adenines are found in the loop, two of which, A_5 and A_6, are protected by viomycin. Viomycin is a competitive inhibitor of group I intron self-splicing, and one contact site on the intron RNA was shown to be the guanosine-binding site [4], which is located in the P7 stem, a pseudoknot in the core of the ribozyme [32,33]. Another ribozyme, which is inhibited by viomycin and whose structure is proposed to be a pseudoknot, is derived from the human HDV RNA [8,34,35]. Further structural characterization of these pseudoknots will have to be undertaken to gain a better understanding of the commonalities of the viomycin-binding sites. The function of RNA pseudoknots is, as yet, unclear, but they are mostly located in flexible and essential parts of RNA molecules (reviewed in [36]). Thus, taken together, the results of our selection and the fact that the natural target sites for viomycin are composed of RNA pseudoknots suggest that this peptide antibiotic has a specificity for, and is able to recognize, particular pseudoknots.

Significance

Viomycin is a small cyclic peptide antibiotic containing the amino acids arginine, serine and lysine, of which all are known to occur in functional domains of RNA-binding proteins. Viomycin inhibits translation and splicing of group I introns and it induces RNA–RNA interactions. To gain a better understanding of the basic principles underlying binding and recognition of viomycin by RNA, we used *in vitro* selection to isolate a variety of viomycin-binding RNA molecules. The selected RNA molecules shared one commonly recurring motif, a pseudoknot, which is important for binding viomycin. The K_d values for viomycin were 11–16 μM, comparable with interactions observed for natural viomycin–RNA complexes. Addition of viomycin to the RNA results in protection from chemical modification of bases within the consensus motif and protection of backbone positions from Pb^{2+} cleavage, confirming that this region is involved in viomycin binding. By comparing the natural viomycin target sites with our novel pseudoknot motif, it was noticed that they all fold into pseudoknot structures. Because all the RNA molecules isolated in this selection have the potential to form pseudoknots, we suggest that the binding site for viomycin is embedded in an RNA pseudoknot structure. Our results further demonstrate the advantage of using random sequence RNA molecules for the isolation and characterization of small aptamers with specific ligand-binding affinity. Thus, basic principles can be revealed which would otherwise escape our attention due to the complexity of the natural antibiotic targets.

Materials and methods

Viomycin affinity chromatography selection procedure

The selection protocol was modified from a previously described procedure [11]. The original random sequence RNA pool construction was described previously [37]. This pool consisted of degenerate RNA molecules with a core region of 74 nucleotides of random sequence flanked by defined regions (total length 113 nucleotides) to allow PCR amplification. The initial complexity of the pool was ~10^{15} different molecules.

Affinity-matrix chromatography: the ligand viomycin (obtained as the sulphate from the Sigma Chemical Company) was immobilized on epoxy-activated Sepharose 6B (purchased from Pharmacia Biotech) following the manufacturer's recommendations. The concentration of covalently-coupled ligand was estimated to be 1 mM by monitoring the UV chromophore of viomycin. The affinity chromatography column was equilibrated in selection buffer (5 mM $MgCl_2$, 50 mM Tris-HCl pH 7.6, 250 mM NaCl), the bed volume of the viomycin-derivatized sepharose used throughout the selection was 1 ml.

Selection procedure: ^{32}P-labelled RNA in selection buffer was applied to the viomycin-derivatized sepharose. The chromatography column was rinsed with selection buffer prior to the elution of RNA molecules, specifically binding viomycin, with affinity buffer (selection buffer containing 2.5 mM viomycin; Table 1). The RNA molecules specifically eluted with viomycin were converted to DNA, amplified by PCR, and transcribed into RNA. This set of procedures constitutes one selection cycle. The resultant purified RNA was the input for the subsequent round of selection. In order to avoid the inadvertent selection of matrix-binding or non-specifically-binding RNA molecules, and to maximize the enrichment of RNA molecules recognizing viomycin with high-affinity and specificity, precautions were undertaken as previously described [11].

Equilibrium gel filtration

Dissociation constants (K_d) were determined in solution using the method of equilibrium gel filtration [38]. Viomycin was radioactively-labelled as described [39] using 20 μmol of viomycin (Sigma) and 20 μmol ^{14}C-urea (Amersham). After labelling, viomycin was separated from urea by a Sephadex G10 column. To verify that the urea label was incorporated into the viomycin, splicing inhibition and oligomerization induction assays were performed (data not shown and [4,40]). RNA (470 pmol) was suspended in buffer (50 μl; 5 mM $MgCl_2$, 50 mM Tris-HCl pH 7.4, 50 mM NaCl unless otherwise indicated) containing ^{14}C-labelled viomycin (5 μM) and was applied to a Sephadex G25 Superfine gel column (Pharmacia Biotech; 8 mm corresponding to 1.6 ml). The position of the RNA elution peak was verified with radioactively-labelled RNA and unlabelled viomycin. The radioactivity of the individual fractions (39.4 μl) was quantified by scintillation counting. The amount of viomycin bound to the selected RNA molecules was determined by calculating the area under the peak, which corresponds to the viomycin–RNA complex. The resultant K_d values were determined from the formula: $K_a = [S \times L] / ([S] \times [L])$, where $[S \times L]$ is the fraction bound in the elution volume ($mol\,l^{-1}$), $[S]$ = concentration of RNA in the elution volume ($mol\,l^{-1}$), and $[L]$ is the concentration of the ligand in the elution volume in ($mol\,l^{-1}$). Experiments were done at least in triplicate.

Chemical modification experiments

Chemical modification of RNA was carried out principally as previously described [11]. The chemical modification agents included: DMS which methylates the base-pairing positions N1 of adenine, N3 of cytosine and also the guanine N7 position; kethoxal, which modifies the positions N1 and N2 of guanine; and CMCT, which modifies the N1 and N3 positions of guanine and uracil, respectively. Minor alterations to this reported protocol were as follows: the binding buffer contained NaCl in place of NH_4Cl, 10 pmol of RNA was used, and the CMCT solution was 80 mg ml^{-1}.

Pb^{2+}-catalyzed cleavage reactions

5′-End-labelled RNA (~0.5 pmol) was equilibrated in buffer (50 mM Tris-HCl pH 7.7, 5 mM $MgCl_2$, and either 50 mM or 200 mM NaCl) and viomycin (100 μM, 200 μM or 500 μM) for 5 min at room temperature (r.t.). Cleavage reactions were initiated by the addition of $Pb(OAc)_2$ (final concentration 0.5 mM in reaction volume 50 μl). After incubation, 30 min at r.t., the reaction was stopped by the addition of STOP solution (1 μl; 1 μg μl^{-1} glycogen and 250 mM EDTA). The products were recovered by ethanol precipitation, dissolved in loading buffer (7 μl; 7 M urea / 1 × TBE, 0.25% bromophenol blue and 0.25% xylene cyanol) and the cleavage reactions were analyzed by electrophoresis. Typically 8% or 10% polyacrylamide gels (1:20) were used, but for the truncated RNA molecules, 20% was used. The T1 digestion ladder was obtained by incubating 5′-end-labelled RNA with RNase T1 (1 μl; 5 units μl^{-1}; Boehringer Mannheim GmbH, Germany) in 7 μl loading buffer containing tRNA (1 μl; 1.5 μg μl^{-1}) for 10 min at 50°C. Quantification of the cleavage products was performed using a Molecular Dynamics Phosphorimager.

Acknowledgements

We are grateful to Eric Westhof for spotting the pseudoknot, to the members of the Schroeder group for helpful discussions and to Martin Egli for critically reading the manuscript. We also thank the students from the genetics III course (Christina Waldsich, Ulli Mückstein, Andrea Dorfleutner and Sandra Buczolits) for providing Figure 6c. This work was supported by the European Community grant number Bio2 CT0345 to R.S. and M.F. and by the Austrian Science Foundation FWF number 9789 and 10615 to R.S.

References

1. Cundliffe, E. (1990). Recognition sites for antibiotics within rRNA. In *The Ribosome*. (Hill, W.E., Dahlberg, A., Garrett, R., Moore, P., Schlessinger, D. & Warner, J., eds), pp. 479–490, ASM, Washington, USA.
2. Von Ahsen, U., Davies, J. & Schroeder, R. (1991). Antibiotic inhibition of group I ribozyme function. *Nature* **353**, 368–370.
3. Von Ahsen, U., Davies, J. & Schroeder, R. (1992). Non-competitive inhibition of group I intron RNA self-splicing by aminoglycoside antibiotics. *J. Mol. Biol.* **226**, 935–941.
4. Wank, H., Rogers, J., Davies, J. & Schroeder, R. (1994). Peptide antibiotics of the tuberactinomycin family as inhibitors of group I intron RNA splicing. *J. Mol. Biol.* **236**, 1001–1010.
5. Rogers, J. & Davies, J. (1994). The pseudodisaccharides: a novel class of group I intron splicing inhibitors. *Nucleic Acids Res.* **22**, 4983–4988.
6. Olive, J.E., *et al.*, & Collins, R.A. (1995). Enhancement of Neurospora VS ribozyme cleavage by tuberactinomycin antibiotics. *EMBO J.* **14**, 3247–3251.
7. Wank, H. & Schroeder, R. (1996). Antibiotic induced oligomerization of group I intron RNA. *J. Mol. Biol.* **258**, 53–61.
8. Rogers, J., Chang, A.H., Von Ahsen, U., Schroeder, R. & Davies, J. (1996). Inhibition of the self-cleavage reaction of the human hepatitis delta virus ribozyme by antibiotics. *J. Mol. Biol.* **259**, 916–925.
9. Schroeder, R. & Von Ahsen, U. (1996). Interaction of aminoglycoside antibiotics with RNA. In *Nucleic Acids and Molecular Biology*. (Eckstein, F. & Lilley, D.M.J., eds), pp. 53–74, Springer-Verlag, Heidelberg, Berlin, Germany.
10. Gold, L., Polisky, B., Uhlenbeck, O. & Yarus, M. (1995). Diversity of oligonucleotide functions. *Annu. Rev. Biochem.* **64**, 763–797.
11. Wallis, M.G., Von Ahsen, U., Schroeder, R. & Famulok, M. (1995). A novel RNA motif for neomycin recognition. *Chem. Biol.* **2**, 543–552.
12. Wang, Y. & Rando, R.R. (1995). Specific binding of aminoglycoside antibiotics to RNA. *Chem. Biol.* **2**, 281–290.
13. Lato, S.M., Boles, A.R. & Ellington, A.D. (1995). *In vitro* selection of RNA lectins: using combinatorial chemistry to interpret ribozyme evolution. *Chem. Biol.* **2**, 291–303.
14. Purohit, P. & Stern, S. (1994). Interactions of a small RNA with antibiotics and RNA ligands of the 30S subunit. *Nature* **370**, 659–662.
15. Schroeder, R. (1994). Dissecting RNA function. *Nature* **370**, 597–598.
16. Laing, L.G. & Draper, D.E. (1994). Thermodynamics of RNA folding in a conserved ribosomal RNA domain. *J. Mol. Biol.* **237**, 560–576.
17. Davies, J. (1994). Inactivation of antibiotics and the dissemination of resistance genes. *Science* **264**, 375–382.
18. Burgstaller, P. & Famulok, M. (1994). Isolation of RNA aptamers for biological cofactors by *in vitro* selection. *Angew. Chem. Int. Ed. Engl.* **33**, 1084–1087.
19. Zuker, M., Jaeger, J.A. & Turner, D.H. (1991). A comparison of optimal and suboptimal RNA secondary structures predicted by free energy minimization with structures determined by phylogenetic comparison. *Nucleic Acids Res.* **19**, 2707–2714.
20. Stern, S., Moazed, D. & Noller, H.F. (1988). Structural analysis of RNA using chemical and enzymatic probing monitored by primer extension. *Methods Enzymol.* **164**, 481–489.
21. Gornicki, P., *et al.*, & Ehresmann, C. (1989). Use of lead(II) to probe the structure of large RNAs. Conformation of the 3′ terminal domain of *E. coli* 16S rRNA and its involvement in building the tRNA binding sites. *J. Biomol. Struct. Dynam.* **6**, 971–984.
22. Puglisi, J.D., Wyatt, J.R. & Tinocco, I.J. (1991). RNA pseudoknots. *Accts. Chem. Res.* **24**, 152–158.
23. Westhof, E. & Jaeger, L. (1992). RNA pseudoknots. *Curr. Opin. Struct. Biol.* **2**, 327–333.
24. Kusmierek, J.T. & Singer, B. (1976). Sites of alkylation of poly(U) by agents of varying carcinogenicity and stability of products. *Biochim. Biophys. Acta* **442**, 420–431.
25. Streicher, B., Von Ahsen, U. & Schroeder, R. (1993). Lead cleavage sites in the core of group I intron-RNA. *Nucleic Acids Res.* **21**, 311–317.
26. Powers, T. & Noller, H. (1994). Selective perturbation of G530 of 16S rRNA by translational miscoding agents and a streptomycin-dependence mutation in protein S12. *J. Mol. Biol.* **235**, 156–172.
27. Moazed, D. & Noller, H.F. (1987). Chloramphenicol, erythromycin, carbomycin and vernamycin B protect overlapping sites in the peptidyl transferase region of 23S ribosomal RNA. *Biochimie* **69**, 879–884.
28. Modolell, J. & Vazquez, D. (1977). The inhibition of ribosomal translocation by viomycin. *Eur. J. Biochem.* **81**, 491–497.
29. Liou, Y.F. & Tanaka, N. (1976). Dual actions of viomycin on the ribosomal functions. *Biochem. Biophys. Res. Commun.* **71**, 477–483.
30. Hornig, H., Woolley, P. & Luhrmann, R. (1983). Effect of codon shortening and the antibiotics viomycin and sparsomycin upon the behaviour of bound aminoacyl-tRNA. Decoding at the ribosomal A site. *FEBS Lett.* **156**, 311–315.
31. Masquida, B., Felden, B. & Westhof, E. (1997). Context dependent RNA–RNA recognition in a three-dimensional model of the 16S rRNA core. *Bioorg. Med. Chem.*, in press.
32. Michel, F., Hanna, M., Green, R., Bartel, D.P. & Szostak, J.W. (1989). The guanosine binding site of the Tetrahymena ribozyme. *Nature* **342**, 391–395.
33. Michel, F. & Westhof, E. (1990). Modelling of the three-dimensional architecture of group I catalytic introns based on comparative sequence analysis. *J. Mol. Biol.* **216**, 585–610.
34. Perrotta, A.T. & Been, M.D. (1991). A pseudoknot-like structure required for efficient self-cleavage of hepatitis delta virus RNA. *Nature* **350**, 434–436.
35. Tanner, N.K., Schaff, S., Thill, G., Petit Koskas, E., Crain Denoyelle, A.M. & Westhof, E. (1994). A three-dimensional model of hepatitis delta virus ribozyme based on biochemical and mutational analyses. *Curr. Biol.* **4**, 488–498.
36. Dam, E., Pleij, K. & Draper, D. (1992). Structural and functional aspects of RNA pseudoknots. *Biochemistry* **31**, 11665–11676.
37. Famulok, M. (1994). Molecular recognition of amino acids by RNA-aptamers: an L-citrulline binding RNA motif and its evolution into an L-arginine binder. *J. Am. Chem. Soc.* **116**, 1698–1706.
38. Hummel, J.P. & Dreyer, W.J. (1962). Measurement of protein-binding phenomena by gel filtration. *Biochim. Biophys. Acta* **63**, 530–532.
39. Misumi, M. & Tanaka, N. (1978). Binding of (^{14}C)tuberactinomycin O, an antibiotic closely related to viomycin, to the bacterial ribosome. *Biochem. Biophys. Res. Commun.* **82**, 971–976.
40. Wank, H. (1996). Interactions of tuberactinomycins with group I intron RNA. PhD thesis, University of Vienna, Austria.